Journal of Experimental Botany, Vol. 59, No. 12, pp. 3425–3434, 2008
doi:10.1093/jxb/ern191 Advance Access publication 24 July, 2008
This paper is available online free of all access charges (see http://jxb.oxfordjournals.org/open_access.html for further details)

Journal of Experimental Botany
www.jxb.oxfordjournals.org

RESEARCH PAPER

Nectar formation and floral nectary anatomy of *Anigozanthos flavidus*: a combined magnetic resonance imaging and spectroscopy study

Michael Wenzler[1], Dirk Hölscher[1], Thomas Oerther[2] and Bernd Schneider[1,*]

[1] *Max-Planck-Institute for Chemical Ecology, Beutenberg Campus, Hans-Knöll-Str. 8, D-07745 Jena, Germany*

[2] *Bruker BioSpin GmbH, Silberstreifen 4, D-76287 Rheinstetten, Germany*

Received 25 March 2008; Revised 9 June 2008; Accepted 30 June 2008

Abstract

Metabolic processes underlying the formation of floral nectar carbohydrates, especially the generation of the proportions of fructose, glucose, and sucrose, are important for understanding ecological plant–pollinator interactions. The ratio of sucrose-derived hexoses, fructose and glucose, in the floral nectar of *Anigozanthos flavidus* (Haemodoraceae) was observed to be different from 1:1, which cannot be explained by the simple action of invertases. Various NMR techniques were used to investigate how such an unbalanced ratio of the two nectar hexoses can be formed. High-resolution ^{13}C NMR spectroscopy in solution was used to determine the proportion of carbohydrates in vascular bundles of excised inflorescences fed with ^{13}C-labelled carbohydrates. These experiments verified that feeding did not affect the metabolic processes involved in nectar formation. *In vivo* magnetic resonance imaging (e.g. cyclic *J* cross-polarization) was used to detect carbohydrates in vascular bundles and ^{1}H spin echo imaging non-invasively displayed the architecture of tepal nectaries and showed how they are connected to the vascular bundles. A model of the carbohydrate metabolism involved in forming *A. flavidus* floral nectar was established. Sucrose from the vascular bundles is not directly secreted into the lumen of the nectary but, either before or after invertase-catalysed hydrolyses, taken up by nectary cells and cycled at least partly through glycolysis, gluconeogenesis, and the pentose phosphate pathway. Secretion of the two hexoses in the cytosolic proportion could elegantly explain the observed fructose:glucose ratio of the nectar.

Key words: *Anigozanthos flavidus*, carbohydrate transport, ^{13}C chemical shift imaging, cryo probe, floral nectar, Haemodoraceae, microimaging, MRI, NMR.

Introduction

The chemical composition of nectar is of immense ecological importance, especially for plant–pollinator interaction. The concentrations and relative proportions of sugars, amino acids, and other nectar components are specifically adapted to the requirements of the pollinator type and therefore show substantial chemical diversity (Elisens and Freeman, 1988; Baker and Baker, 1990; Cronk and Ojeda, 2008). Moreover, the evolutionary origin and architecture of nectaries are as diverse as the nectar supply seems to be.

Despite a plethora of publications about nectaries, nectar formation and nectar composition (reviewed, for example, by Lüttge, 1961; Fahn, 1979, 2000; Pacini *et al*., 2003; De la Barrera and Nobel, 2004), the mechanisms determining nectar composition are not yet fully understood. The ultrastructural and cell-specific localization of the processes involved in generating nectar is similarly unclear. Nectaries should not be assumed always to be capable of fine-tuning the chemical composition of the nectar; in some plants, they may function only as tissue secreting phloem sap. Relatively little is known about the genetic background of nectary differentiation or the regulation of nectar production. Only one gene (*NEC1*) thought to be involved in the nectary differentiation has been described (Ge *et al*., 2000). Two nectar quantitative

* To whom correspondence should be addressed. E-mail: Schneider@ice.mpg.de

Abbreviations: α-glcp, α-D-glucopyranose; β-fruf, β-D-fructofuranose; β-frup, β-D-fructopyranose; β-glcp, β-D-glucopyranose; CSI, chemical shift imaging; MRI, magnetic resonance imaging; NMR, nuclear magnetic resonance; NOE, nuclear Overhauser effect; QTL, quantitative trait loci.

trait loci (QTL), that help control the amount of nectar produced, have been identified in *Mimulus* and *Petunia* (Bradshaw *et al*., 1995; Stuurman *et al*., 2004). In *Petunia*, Stuurman *et al*. (2004) found another QTL; this controls the ratio of hexoses to sucrose, which may coincide with invertase activity. Invertase-catalysed hydrolysis of sucrose seems to be responsible for the ratio of hexoses to sucrose (Nicolson and Fleming, 2003) in the nectar. However, the simple action of invertase should result in a glucose-to-fructose ratio of 1:1, which is not always the case (Baker *et al*., 1998; Chalcoff *et al*., 2006; Wolff, 2006; Hölscher *et al*., 2008). Hence, additional enzymes and transporters must be involved in generating the chemical composition of nectars. Acidic phosphatases have been reported to play a role in nectar secretion (Ziegler, 1956).

The nectar composition of many plants has been studied for more than 50 years using various chromatographic and spectroscopic techniques. In a recent study, nuclear magnetic resonance (NMR) spectroscopy was used for metabolic profiling of *Anigozanthos* floral nectar (Hölscher *et al*., 2008). ^{13}C NMR was used to determine the major carbohydrates quantitatively, which in this nectar are glucose and fructose. Sucrose, which usually is one of the major sugars in nectar, was detected in low concentrations, together with other minor nectar components such as amino acids only by using the much more sensitive ^{1}H NMR spectroscopy. In addition to the very low sucrose level, interestingly, the *Anigozanthos* floral nectar was found to contain glucose and fructose in a ratio of 1.2:1.0 (Hölscher *et al*., 2008).

The observation of a glucose-to-fructose ratio different from 1:1 prompted the present work. NMR spectroscopy and magnetic resonance imaging (MRI) were used to investigate both nectar formation and the anatomy of the nectary. In contrast to light and electron microscopy, the usual methods for studying the architecture of nectaries (Figier, 1968; Simpson, 1993), MRI is non-destructive. It requires only limited sample preparation and avoids artefacts. The cyclic *J* cross-polarization MRI method developed and demonstrated on castor bean seedlings by Heidenreich *et al*. (1998) was used in the present study to observe the sugar composition and distribution in the vascular bundles of excised inflorescences of *Anigozanthos flavidus*. Another aim was to validate excised inflorescences as a model system, especially to verify if experimental manipulation, for example, feeding ^{13}C-labelled carbohydrates, affects the metabolic processes involved in nectar formation. In this study excised inflorescences of *A. flavidus* were used for precursor feeding experiments and single flowers for MRI. *A. flavidus*, a Haemodoraceae native to Southwestern Australia, is interesting due to the accumulation of phenylphenalenones and other secondary metabolites with ecological implications.

Materials and methods

Plant material

Plants of *A. flavidus* DC. were raised from seeds (Chiltern Seeds, Bortree Stile, UK) and grown in soil in the greenhouse. The temperature was 20–24 °C during the day and 18–21 °C during the night. Relative air humidity was between 60% and 70%. The natural daily photoperiod was supported with 16 h illumination from Phillips Sun-T Agro 400 Na lights.

Labelled compounds

[U-^{13}C]glucose (99% ^{13}C) and [1-^{13}C]fructose (99% ^{13}C) were from Deutero GmbH, Kastellaun, Germany.

Light microscopy

Peduncles of *A. flavidus* were cut with a razor blade (Dovo Merkur, Solingen, Germany) to get extra-thin hand-made sections. The sections were made at ×40 magnification (objective Leica 506074 C Plan 4×/0.10) on a Leica DM6000B light microscopy system.

Feeding experiments

For nectar collection experiments, excised inflorescences of *A. flavidus* were allowed to take up [U-^{13}C]glucose or [1-^{13}C]fructose hydroponically from 20 mM and 25 mM aqueous solutions, respectively. Nectar was collected twice from each flower 24 h and 48 h after transfer of the excised inflorescences to the feeding solutions. For all other labelling experiments, cut *A. flavidus* flowers were fed overnight in 10–500 mM solutions of [U-^{13}C]glucose or 5 mM solutions of [1-^{13}C]fructose.

Nectar collection and sample preparation

In the feeding experiments, approximately 15 µl nectar per flower was collected with Eppendorf tips from inflorescences of *A. flavidus*. In the [U-^{13}C]glucose feeding experiment, 30 µl nectar was dissolved in 500 µl D_2O and subjected to ^{13}C NMR. In the [1-^{13}C]fructose feeding experiment 80 µl nectar was dissolved in 600 µl D_2O and evaporated to dryness under a stream of N_2 gas to remove H_2O. This procedure was repeated once. Finally, the sample was subjected to NMR analysis in D_2O. At the start of the feeding experiments, all nectar present in the flowers was collected, subjected to the same sample preparation as described above and used as a reference.

NMR

^{1}H and ^{13}C NMR data were recorded on a Bruker AVANCE 400 spectrometer operating at a ^{1}H frequency of 400.13 MHz and a ^{13}C frequency of 100.61 MHz, respectively. All spectra were recorded in D_2O at 25 °C. ^{1}H NMR spectra were measured with presaturation of the HDO signal. ^{13}C NMR experiments were executed using power gated decoupling. 3-(Trimethylsilyl) 2,2,3,3-tetradeuteropropionic acid (TSP) was used as an internal standard for referencing ^{1}H NMR spectra.

Magnetic resonance imaging/chemical shift imaging

All experiments were carried out on Bruker AVANCE 400 spectrometers equipped with Bruker microimaging systems. ^{1}H spin echo images of flowers were acquired using a 'Micro 5' RT-probe with an exchangeable 5 mm coil insert. A ^{1}H^{13}C cyclic *J* cross-polarization image (Heidenreich *et al*., 1998) of a 5 mm slice of a flower peduncle 18 mm above the cutting site was acquired using a cryogenic microimaging probe at the facilities of Bruker

Rheinstetten. The excised inflorescence was placed in a 5 mm NMR tube with 50 µl of a 500 mM [U-^{13}C]glucose solution. For the cross-polarization image the ^{1}H^{13}C cross signal (δ 5.23/93.2) of C-1 of glucose in the sucrose and of α-glucose was selected.

^{13}C NMR chemical shifts of glucose and fructose

^{13}C NMR signals were assigned according to Kalinowski *et al.* (1984): δ 102.6 (C-2, β-fruf), δ 99.2 (C-2, β-frup), δ 97.0 (C-1, β-glcp), δ 93.2 (C-1, α-glcp), δ 81.7 (C-5, β-fruf), δ 77.0, 76.9 (C-3, C-5 β-glcp), δ 76.5 (C-3, β-fruf), δ 75.6 (C-4, β-fruf), δ 75.3 (C-2, β-glcp), δ 73.9 (C-3, α-glcp), δ 72.6, 72.5 (C-2, C-5, α-glcp), δ 70.8 (C-4, β-frup), δ 70.75 (C-4, α-glcp), δ 70.7 (C-4, β-glcp), δ 70.3 (C-5, β-frup), δ 68.7 (C-3 β-frup), δ 65.0 (C-1, β-frup), δ 64.4 (C-6, β-frup), δ 63.8 (C-1, β-fruf), δ 63.5 (C-6, β-fruf), δ 61.9 (C-6, β-glcp), δ 61.7 (C-6, α-glcp).

Results

Labelling experiments to observe carbohydrate conversion in vascular bundles

To gain a better understanding of the processes generating the relative proportion of the nectar carbohydrates, hydroponic feeding experiments with [1-^{13}C]fructose and [U-^{13}C]glucose, respectively, were carried out using excised inflorescences of *A. flavidus*. The nectar, collected 24 h and 48 h after the inflorescences were transferred into the feeding solutions with the labelled compounds, was dissolved in D_2O and analysed without further treatment by ^{13}C NMR unless otherwise noted. Signals of α- and β-D-glucopyranose (α-glcp, β-glcp), β-fructopyranose (β-frup), and β-fructofuranose (β-fruf) were assigned in compliance with the literature (Kalinowski *et al.*, 1984). Mixtures of known glucose-to-fructose ratios were used as references to determine the glucose-to-fructose ratio of floral nectar from untreated intact plants (Hölscher *et al.*, 2008), i.e. plants which were not subjected to feeding experiments. This method allowed errors due to different relaxation effects and NOE enhancement of different carbons to be avoided. In the [U-^{13}C]glucose feeding experiment, the glucose-to-fructose ratio was determined based on the integrals of C-1 and C-6 signals of fructose and glucose. Overlapping multiplets of C-2 to C-5, caused by ^{13}C-^{13}C coupling, were not used for integration. All signals except that of C-1, from which some label may be lost due to decarboxylation in the pentose phosphate pathway, were used for integration in the [1-^{13}C]fructose feeding experiments. In the [1-^{13}C]fructose as well as in the [U-^{13}C]glucose feeding experiments, a glucose-to-fructose ratio of approximately 1.2:1 was found which is identical with that observed in nectar from untreated plants. Sucrose was not detectable in the nectar using ^{13}C NMR. In the [1-^{13}C]fructose feeding experiment, the ^{13}C abundance at C-1 in α- and β-glcp could be determined from the satellites of their well-resolved signals at δ 5.234 and δ 4.647 in the ^{1}H NMR spectrum as 4.8% (label+natural abundance). The natural ^{13}C abundance of the nectar glucose was determined as 1.2% using the nectar sampled at the start of the [1-^{13}C]fructose feeding experiment. Analysing ^{13}C NMR spectra gave a ratio of ^{13}C label of C-1 to C-6 of 3.5:1 for α- and β-glcp and of 4.8:1 for β-fruf and β-frup. For positions C-2 to C-5, no significant incorporation of ^{13}C label was observed. The fraction of ^{13}C-labelled hexoses in the [1-^{13}C]fructose feeding experiment is around 5%. In the hexoses obtained from the [U-^{13}C]glucose feeding experiments, the C-1 signals of α- and β-glcp of ^{13}C-labelled glucose appear as doublets due to ^{13}C^{13}C coupling ($J_{C\text{-}1\text{–}C\text{-}2}$=45.6 Hz). In contrast, the C-1 signals of the unlabelled glucose appear as central singlets between the doublet lines (Fig. 1). The proportion of labelled and unlabelled glucose was determined from the integral ratio of the doublet and central singlet. Taking into account the natural abundance of ^{13}C in the nectar hexoses of 1.2%, the fraction of ^{13}C-labelled hexoses was determined to be approximately 8%.

The finding that the carbohydrate composition, i.e. the glucose-to-fructose ratio, of *Anigozanthos* nectar is not affected by ^{13}C-labelled glucose or fructose feeding raised the question, what happens during the uptake and transport of the carbohydrates in cut inflorescences? To answer this, overnight feeding experiments of excised *Anigozanthos* inflorescences with 5 mM [1-^{13}C]fructose or different concentrated solutions of [U-^{13}C]glucose (10, 100, and 200 mM), respectively, were performed. After discarding 5 mm of the bottom end of the peduncle, which was immersed in the feeding solution, segments approximately 15 mm long from different positions in the peduncle were ground in liquid nitrogen, extracted with methanol, and subjected to ^{13}C NMR. In segments taken from directly

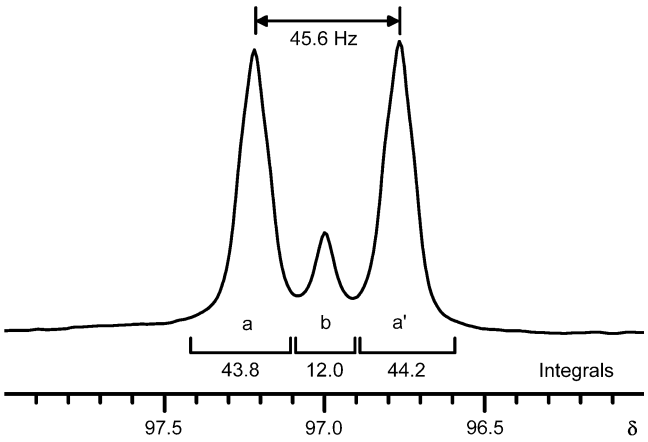

Fig. 1. Partial ^{13}C NMR spectrum of *Anigozanthos flavidus* nectar obtained from the [U-^{13}C]glucose feeding experiment, showing the C-1 signal of β-D-glucopyranose. Due to ^{13}C^{13}C coupling $J_{C\text{-}1\text{–}C\text{-}2}$=45.6 Hz (indicated above the signal) the C-1 signal of [U-^{13}C]glucopyranose appears as a doublet (a+a′), whereas the C-1 signal of unlabelled β-D-glucopyranose appears as a central singlet (b). Integration of these signals leads to a ratio of ^{13}C-labelled to unlabelled hexoses of (a+a′):b = 88:12.

below the flower, the only carbohydrate signals in the spectrum of 5 mM [1-^{13}C]fructose feeding were that of the glucose (δ 93.0) and fructose (δ 62.1) moieties of sucrose (Fig. 2). The signals at δ 72.7, δ 67.6, and δ 67.0 were assigned to shikimic acid using two-dimensional ^{1}H^{13}C heterocorrelation NMR spectroscopy, especially the heteronuclear single quantum coherence (HSQC) experiment, which unambiguously reveals the connectivity between ^{13}C and ^{1}H resonances. In the spectra of 10 mM and 100 mM [U-^{13}C]glucose feeding, only signals of sucrose (split due to ^{13}C^{13}C couplings between isotopically enriched carbon positions, thereby making the spectrum more complex) and of shikimic acid were present. An additional signal in the spectrum of 200 mM glucose feeding at δ 97.0 (C-1, β-glcp) and a tiny signal at δ 99.2 (C-2, β-frup) showed that free glucose and fructose were present. From these data it was concluded that for fructose (5 mM) and glucose concentrations up to 100 mM, the two hexoses are completely transformed to sucrose during uptake into the peduncle and transport to the flower.

Extracts of peduncle segments taken from different positions below the flower were used to investigate the relationship between hexose transformation and the distance of the cutting site. As distance from the cutting site increased, the C-1 signal of β-glcp (δ 97.0) decreased in feeding experiments with 100 mM (Fig. 3) and 200 mM [U-^{13}C]glucose. In feeding experiments with 100 mM glucose 40 mm away from the cutting site (corresponding to the top segment below the flower), no signals of β-glcp but all signals of sucrose were detectable in the ^{13}C NMR spectrum.

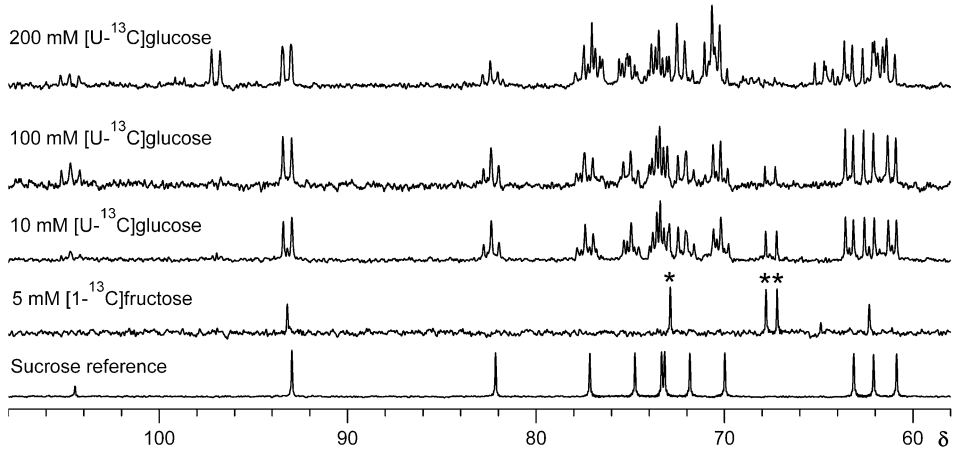

Fig. 2. ^{13}C NMR spectra of methanol extracts of peduncles (15 mm-long segments positioned directly below the flower) after *Anigozanthos* inflorescences were fed overnight with 5 mM [1-^{13}C]fructose and 10, 100, and 200 mM [U-^{13}C]glucose, respectively. A spectrum of sucrose is shown as a reference. In the spectra of fructose feeding and 10 mM and 100 mM glucose feeding, only signals of sucrose and shikimic acid (marked by asterisks) are present. Additional signals at δ 99.2 (very small) and δ 97.0 in the spectrum of 200 mM glucose feeding are attributable to C-2 of β-D-fructopyranose and C-1 of β-D-glucopyranose, respectively.

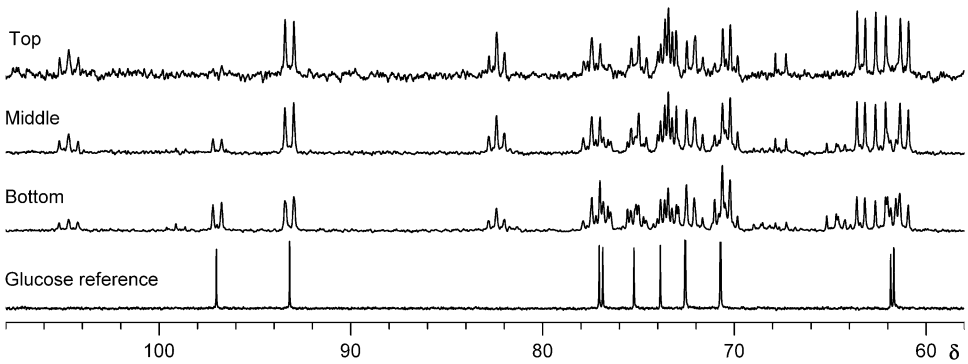

Fig. 3. ^{13}C NMR spectra of methanol extracts of different sections of *Anigozanthos* peduncles after inflorescences were fed overnight with 100 mM [U-^{13}C]glucose. Before extraction with methanol, the 70 mm-long peduncle was divided into three segments (top 0–30 mm, middle 30–52 mm, and bottom >52 mm below the flower). A spectrum of unlabelled glucose is shown at the bottom. From bottom to top the signal at δ 97.0 (C-1, β-D-glucopyranose) decreases. The absence of the C-1 signal of β-D-glucopyranose in the spectra of the top section indicates that all glucose is converted to sucrose during the uptake into and the passage through the peduncle.

Magnetic resonance imaging of sugars in vascular bundles

MRI and chemical shift imaging (CSI) techniques were used to visualize vascular bundles of *A. flavidus* peduncles and the carbohydrates within them. In axial ^{1}H gradient echo images of peduncles, bright round spots are clearly visible (Fig. 4A). Given the position and the shape of these spots, they probably depict vascular bundles. Light microscopic data from a cross-section of the same position of the same peduncle taken after MR imaging substantiated this interpretation (Fig. 4B). Due to magnetic susceptibility effects, the air containing parenchyma in the centre of the peduncle appears black in the gradient echo image. By applying spin echo sequences, this artefact could be avoided (Fig. 4C).

$^{1}H^{13}C$ cyclic *J* cross-polarization imaging (Heidenreich *et al*., 1998) was used to study carbohydrate distribution in the peduncle. After an *Anigozanthos* flower was fed overnight with 500 mM [U-^{13}C]glucose solution, the flower with a 40-mm peduncle was transferred to a 5 mm NMR tube. Since feeding flowers such a highly concentrated glucose solution led to a mixture of glucose and sucrose in the peduncle (Fig. 2), the overlapping $^{1}H^{13}C$ cross-signals of C-1 of α-glcp and the glucose moiety of sucrose were selected for imaging. These parameters made the experiment more sensitive and allowed the distribution of both sugars to be mapped in one experiment. A cross-polarization image of a 5 mm slice 18 mm above the cutting site was superimposed on a ^{1}H spin-echo image of the same slice (Fig. 4D). The position of the sugar signals coincided with that of the vascular bundles, which together with the results from ^{13}C NMR analysis of peduncle segments after feeding inflorescences labelled sugars, led to the conclusion that both glucose and sucrose are located in the transport system of the peduncle. No significant amounts of ^{13}C-labelled sucrose and glucose from the feeding were stored in other peduncle parenchyma tissue.

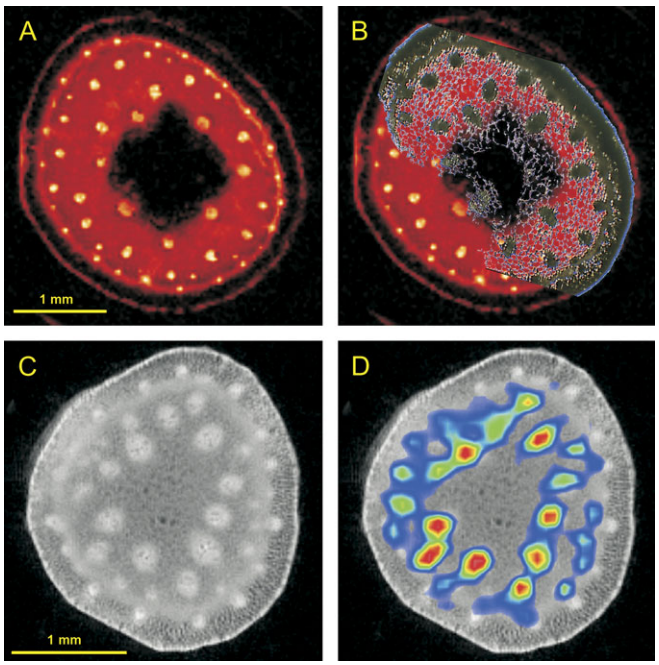

Fig. 4. (A) ^{1}H gradient echo image of an *Anigozanthos flavidus* peduncle (62×62 μm^2 in-plane resolution, 1 mm slice thickness). The bright spots are the vascular bundles. (B) ^{1}H image was overlaid with a light microscopic image from a slice of the same peduncle as in (A) prepared after ^{1}H imaging. (C) ^{1}H spin echo reference image of *A. flavidus* peduncle measured at a cryogenic probe and 400 MHz ^{1}H frequency (32×32 μm^2 in-plane resolution, 1 mm slice thickness) (D) Reference image of (C) overlaid with a cross-polarization image in false colour mode showing the distribution of the $^{1}H^{13}C$ cross-signal of C-1 of α-D-glucopyranose and the glucose moiety of sucrose (156×156 μm^2 in-plane resolution, 5 mm slice thickness, acquisition time 4 h, the signal intensity increases from dark blue over light blue, green, and yellow to red).

Nectary anatomy studies using ^{1}H magnetic resonance microimaging

The anatomy (and phylogeny) of septal nectaries of Haemodoraceae (Grassmann, 1884), including *A. flavidus*, was studied by Simpson (1993) using light microscopy and computer-assisted 3D reconstructions. In the present work, the anatomy of the septal nectaries and especially their connection to the vascular system non-destructively was investigated by applying ^{1}H MRI. ^{1}H spin-echo images were acquired at 400 MHz resonance frequency using a room temperature probe. Intact flowers were placed into a 5 mm NMR tube. ^{1}H spin echo images of a younger (A–L) and an older flower (M–P) of *A. flavidus* are shown in Fig. 5. In the axial slices the main parts of the flower are clearly discernible. The lower part of the flower is surrounded by three tepals that have grown together to form a tube. Inside the tepals the vascular bundles appear as bright spots. In Fig. 5E and F the bifurcation of a vascular bundle is marked by asterisks. The lower part of the flower is divided by three septa, each containing one nectary. In the younger flower, the lumens of the nectaries appears bright, indicating that they are filled with nectar, whereas in the older flowers the lumens are dark but surrounded by a brighter layer. The nectaries open in the cavity at the style base near the apex of the ovary (Fig. 5L).

Coming from the peduncle, the vascular bundles furcate between the tepals and the middle of the flower, where they reach the vicinity of the nectaries and the base of the ovary. In the septa themselves no vascular bundles are discernible.

Discussion

Whether nectar constituents are supplied by phloem or xylem or both has long been a matter of debate. Agthe (1951) showed that the nectaries of *Euphorbia*

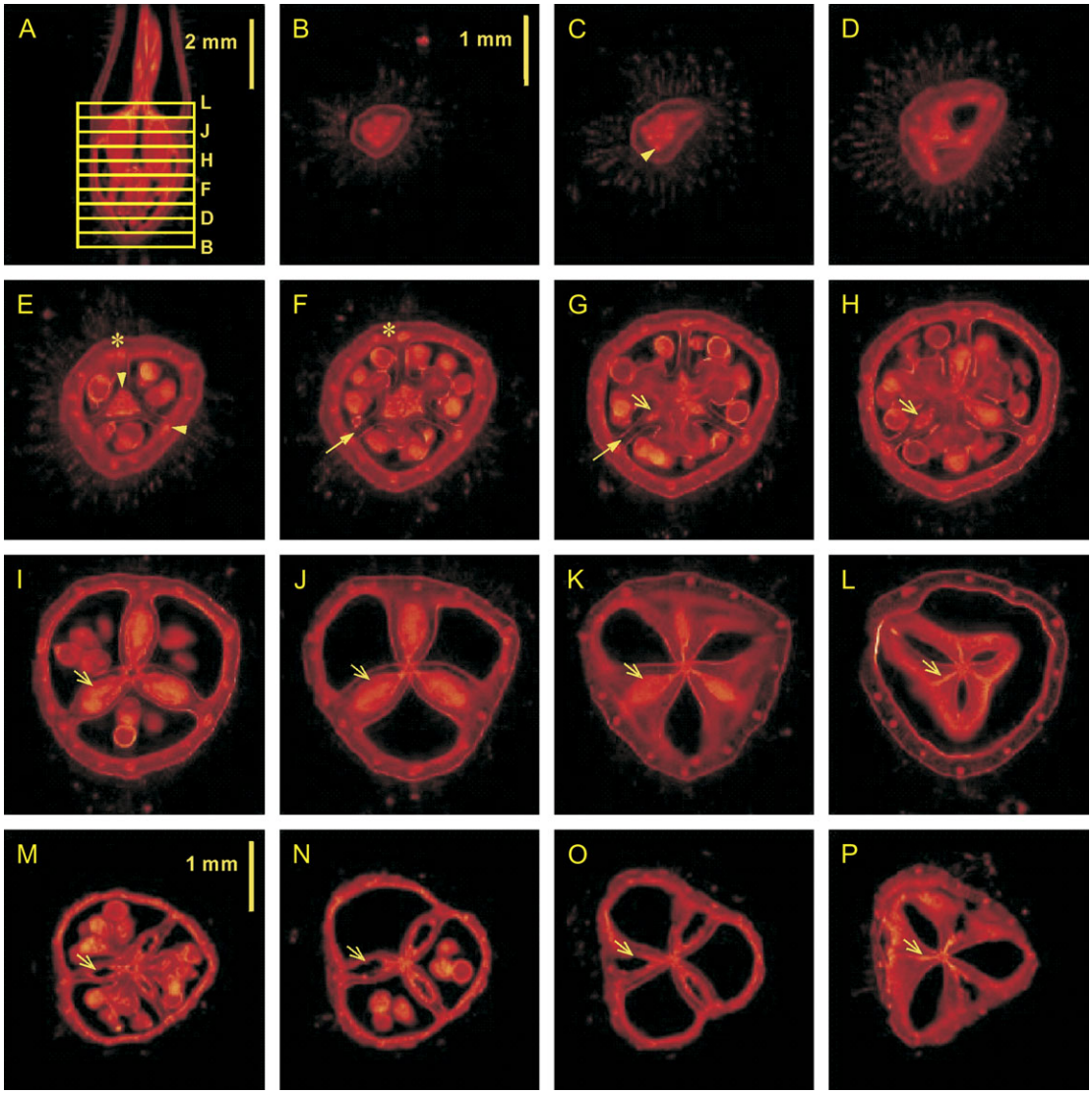

Fig. 5. ^{1}H spin echo images of *Anigozanthos flavidus* flowers at two different developmental stages (slice thickness 150 μm). In the false colour images black corresponds to low signal intensities and brighter colours to higher signal intensities. (B–L) Axial slices of a young flower (30×30 μm^2 in-plane resolution). In (A) the slice positions are shown. (M–P) Axial slices of an older flower (78×78 μm^2 in-plane resolution). Arrow heads indicate some vascular bundles. In (E) and (F) the asterisks mark the branching of a vascular bundle. In (F) and (G) closed arrows indicate the position of septa. One septal nectary in each of the slices (G–P) is marked by an open arrow. In (G–L) the nectaries are filled with nectar, whereas in the older flower shown in slices (M–P), the nectaries have a dark centre, indicating that they are empty.

pulcherrima are connected only to the phloem but not the xylem and concluded that the secreted nectar is pure phloem sap. Later studies confirmed that nectaries are supplied only by phloem (Elias *et al*., 1975; Razem and Davis, 1999). But there are some other examples: in *Ranunculus* sp. the nectaries are supplied by xylem and phloem, in *Fritillaria imperialis* exclusively by xylem (Frey-Wyssling, 1955). Nowadays it is generally accepted that nectar is derived from the phloem solution (De la Barrera and Nobel, 2004). This implies that sucrose, the major carbohydrate in the phloem, is converted at least partially to glucose and fructose to generate the species-specific glucose:fructose:sucrose proportion of floral nectar. Lüttge (1961) assumed that in species where glucose and fructose are present in the nectar, the nectar sugar is secreted as sucrose followed by an extracellular cleavage by invertase. This should result in a glucose:fructose ratio of 1:1. On the other hand, in many nectars the glucose:fructose ratio is quite different from a balanced proportion (Baker *et al*., 1998; Chalcoff *et al*., 2006; Wolff, 2006). In *Anigozanthos manglesii* a glucose:fructose:sucrose ratio of 11:8:1 was reported (Baker *et al*., 1998). Possible explanations for a glucose:fructose ratio that differs from 1:1 include the alteration of nectar by micro-organisms (Lüttge, 1961) or the occurrence of oligosaccharides in the nectar (Lüttge, 1962). No signals

of oligosaccharides could be observed in the NMR spectra of *A. flavidus* nectar, but microbial effects on nectar composition of greenhouse-grown plants cannot be excluded in the present study.

De la Barrera and Nobel (2004) showed that flowers in intact plants are supplied with water via the phloem because of the higher water potential of flowers compared with the leaves. Leaves in intact plants are a source for sugars, which are transported via the phloem. In excised flowers it is not clear if carbohydrates and/or other substances are transported from the cutting site to the flower via the xylem, the phloem, or both (Zimmermann, 1953). Therefore the sugar composition of the nectar was manipulated experimentally in feeding experiments with ^{13}C-labelled glucose and fructose. No alterations of the nectar composition were observed, however. The ^{13}C label proved that the fed sugars are transported to the nectaries and used as a source for nectar production. Although similar amounts and concentrations of ^{13}C-labelled sugars were supplied in parallel feeding experiments, the portion of labelled sugars in the nectar varied greatly between 1% and 8%. Differences of the inflorescences such as age, number, and size of individual flowers are the most likely explanation for this variation.

In glucose and fructose feeding experiments with excised *Impatiens* flowers, whose nectar only contains sucrose, Zimmermann (1953) also did not observe any changes in the nectar composition. He claimed that the glucose and fructose were included in the normal intermediary metabolism. This also seems to be the case for cut *A. flavidus* flowers. For sugar concentrations up to 100 mM in the feeding solution, either all the glucose or all the fructose is transformed into sucrose before reaching the flower. As demonstrated in cyclic *J* polarization experiments, the ^{13}C-labelled sugars are located in the vascular bundles. Using a cryogenically cooled imaging probe, an exceptionally large signal-to-noise ratio and a high in-plane resolution of 156×156 μm was achieved. Thus, compared to measurements with 110×876 μm in-plane resolution done with a conventional room temperature probe for monitoring dynamic changes of the ^{13}C signal intensity in intact castor bean seedlings (Heidenreich *et al*., 1998), considerable progress was made, although the experiments were optimized for different purposes and, in the present study, experimental time was extended to 4 h compared to 1.5 h used by Heidenreich *et al*. (1998). Nevertheless, because the diameter of the vascular bundles is smaller than 300 μm, phloem and xylem cannot be distinguished. To obtain resolved images of phloem and xylem, increasing the in-plane resolution in both dimensions by a factor of at least four would be necessary; doing so would increase the measurement time by a factor of 64 (more than a week), while decreasing the signal-to-noise ratio by a factor of four. Therefore the distribution of sucrose and the two hexoses between the phloem and the xylem, the uptake mechanisms, and the site of sucrose formation remain to be investigated. Kallarackal and Komor (1989), studying *Ricinus communis* seedlings, showed that at low glucose concentrations, glucose is transformed to sucrose before being transported into the sieve elements, but at higher concentrations, unchanged glucose was taken up. Normally the carbohydrate concentration in xylem sap is lower than 0.5%, but in some perennial plants sugar concentrations up to 8% are observed in the early spring (Öpik and Rolfe, 2005). Hence, the possibility that carbohydrates are transported via the xylem in the artificial system used in the present study cannot be excluded. The observed decrease of glucose during the transport through the peduncle (Fig. 3) can be explained by two processes. One is the simple metabolic consumption of glucose in the phloem symplasm, which contains an operational glycolytic pathway (Geigenberger *et al*., 1993). Another is the leaking and retrieval of sugars during phloem transport (Ayre *et al*., 2003) associated with sucrose formation in the parenchyma of the vascular bundles. As a result, for the low sugar concentrations used in the feeding experiments for nectar sampling, all the glucose or fructose was metabolized or transformed into sucrose before reaching the nectaries. Therefore no differences in the nectar composition of untreated intact plants and the nectar in the feeding experiments using excised flowers were observed.

Studying the position of the ^{13}C label in the [1-^{13}C]fructose feeding experiments allowed the pathways in which the fructose is involved to be estimated before the labels appear in sucrose in the vascular bundles and in hexoses in the nectar. In the peduncle extracts from directly below the flowers, only C-1 of the glucose (δ 93.0) and fructose (δ 62.1) moieties of sucrose are enriched with ^{13}C (Fig. 2). This suggests that the fructose is directly phosphorylated, probably after uptake in the parenchyma cells; in addition, half of the fructose-6-phosphate seems to be converted to glucose-6-phosphate and further to UDP-glucose. Both fructose-6-phosphate and UDP-glucose are used to synthesize sucrose, without entering other pathways such as glycolysis and gluconeogenesis. If [1-^{13}C]fructose enters glycolysis, gluconeogenesis and the pentose phosphate pathway, some of the label should be transferred into the C-6 position (Fig. 6). Randomization in carbohydrate metabolism, although in the different context of starch and sucrose biosynthesis, was previously observed in *Solanum tuberosum* and *Vicia faba* (Viola *et al*., 1991).

Unlike the sucrose detected in peduncles, in hexoses found in the nectar the ^{13}C labels were indeed observed in C-1 and C-6 positions. The appearance of the label in C-6 clearly indicates that the sucrose after uptake from the neighbouring vascular bundles into the nectaries must be hydrolysed, so that the hexoses can enter into the glycolysis, gluconeogenesis, and pentose phosphate pathways (Fig. 6).

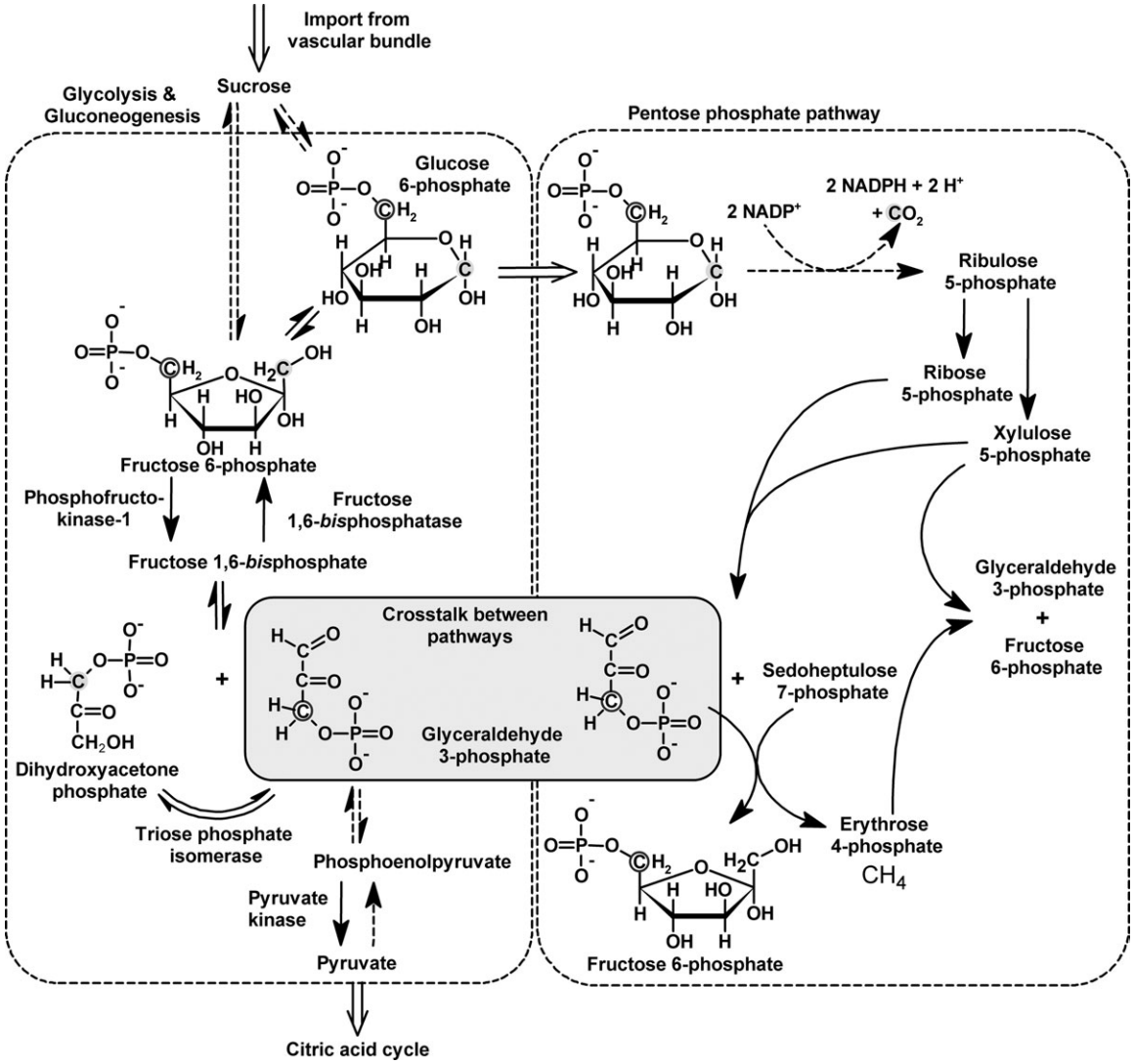

Fig. 6. Hypothetical carbohydrate metabolism in floral nectaries of *Anigozanthos flavidus*. In [1-^{13}C]fructose feeding experiments of inflorescences, the transfer of ^{13}C label from position one to six of hexoses after the transport through the vascular bundles was observed. The only explanation is that the sucrose delivered from the vascular bundle is hydrolysed followed by entering of fructose 6-phosphate and glucose 6-phosphate into glycolysis to generate energy and the pentose phosphate pathway for NADPH formation. The crucial step for the transfer from ^{13}C label of C-1 in the hexoses (highlighted by a grey circle) to C-6 (highlighted by an open circle) is the isomerization between dihydroxyacetone phosphate and glyceraldehyde 3-phosphate and the exchange of [3-^{13}C]glyceraldehyde 3-phosphate between glycolysis and the pentose phosphate pathway. The reaction of [3-^{13}C]glyceraldehyde 3-phosphate with sedoheptulose 7-phosphate leads to erythrose 4-phosphate and [6-^{13}C]fructose 6-phosphate. The latter can be isomerized to [6-^{13}C]glucose 6-phosphate and both could be used as sugars for nectar secretion. The decarboxylation in the beginning of the pentose phosphate pathway leads to a loss of ^{13}C label. This is an elegant explanation for the lower ^{13}C ratio of C-1 to C-6 of glucose in comparison to fructose in the [1-^{13}C]fructose feeding experiment.

The reversible isomerization of glyceraldehyde 3-phosphate to dihydroxyacetone phosphate catalysed by triose phosphate isomerase during glycolysis and gluconeogenesis explains the transfer of some of the label from position C-1 to C-6 in hexoses. Phosphofructokinase-1 and fructose 1,6-*bis*phophatase as key enzymes of glycolysis and gluconeogenesis are reciprocally regulated, so that only one of the two pathways is active. Therefore some of the glucose-6-phosphate probably enters the oxidative part of the pentose phosphate pathway, which produces NADPH and pentose-phosphate, whereas C-1 is removed as CO_2. This elegantly explains the lower ratio of ^{13}C-labelled C-1 to C-6 for glucose (3.5:1) compared with fructose (4.8:1) in the [1-^{13}C]fructose feeding experiments. Some of the hexoses will enter glycolysis. During the regeneration of hexose-phosphate from pentose-phosphate, glyceraldehyde 3-phosphate from the glycolysis pathway (^{13}C-labelled in C-3) can enter the non-oxidative part of the pentose-phosphate pathway which leads to C-6 labelled hexoses. In the present discussion, a so-called traditional model for the glycolysis and pentose phosphate pathways (Kleijn *et al*., 2007) is used. The half reaction

model (Kleijn *et al*., 2007) explains the observed labelling pattern but does not affect the arguments presented in this work. Metabolic flux measurements (Eisenreich *et al*., 2004; Ratcliffe and Shachar-Hill, 2006) would be useful to study the pathways involved in nectar formation quantitatively. Excised flowers of *Anigozanthos* are considered a good model for using this method, since in our feeding experiments the nectar formation is not disturbed.

These results indicate that, in *A. flavidus*, sucrose is not simply transported apoplastically from the vascular bundles into the nectar accompanied by the action of invertases and therefore is not the direct source of nectar sugars. It seems that sucrose, or glucose and fructose after cleavage through (cell-wall bound) invertase, is first taken up by the cells of the nectaries and, at least partly, cycled through the glycolysis, gluconeogenesis, and pentose phosphate pathways as shown in Fig. 6. Glucose and fructose are then most probably secreted through hexose transporters, so that the nectar's glucose-to-fructose ratio simply reflects the equilibrium of these two hexoses or their phosphates in the cytosol of the nectary cells.

Anatomy

In the ^{1}H magnetic resonance microimages, good resolution allows different parts of the flower to be clearly distinguished. MRI does not reach the high resolution of ultrastructural electron microscopic studies (Fahn, 1979). However, it is a non-invasive method and therefore artefacts due to sample preparation can be excluded. By imaging serial 150 μm slices, we could visualize the course of the vascular bundles in the vicinity of the nectaries. The images shown in Fig. 5 support the possibility that the nectaries are directly connected to thin strands of phloem or xylem. These results strengthen the argument that the sugars used for nectar formation are delivered by the vascular bundles and have only a short distance, if any, to bridge, apoplastically or symplastically, when translocated to the nectaries. In old flowers of *A. flavidus* (Fig. 5M–P), the nectaries show a bright layer of tissue surrounding the lumen of the nectaries. This tissue may consist of three to five layers of differentiated cells with densely staining content as described by Simpson (1993) in his light microscopic studies of Haemodoraceae nectaries.

Conclusions

In summary, the present investigations demonstrate that magnetic resonance spectroscopy and imaging techniques are useful tools with which to study processes of nectar formation and anatomy of nectaries. The present study, has led us to establish a model in *Anigozanthos* of carbohydrate transport and metabolism, according to which sucrose is translocated from the vascular bundles to the nectar-secreting epithelial cells in floral nectaries. A portion of the sucrose is processed in these cells through pathways of the intermediary metabolism and hydrolysed to glucose and fructose, which are proportionally secreted to the lumen of the nectary. Peduncles and flowers of *A. flavidus* can be used as model systems to study nectar formation.

Acknowledgements

The authors thank Dieter Gross and Volker Lehmann (Bruker BioSpin, Rheinstetten) for access to a Bruker spectrometer equipped with a cryogenically cooled microimaging probe and expert technical advice. We wish to thank Tamara Krügel and Udo Kornmesser for raising plants. Emily Wheeler (Jena) is acknowledged for editorial assistance.

References

Agthe C. 1951. Über die physiologische Herkunft des Pflanzennektars. *Bericht der schweizerischen botanischen Gesellschaft* **61,** 240–273.

Ayre BG, Keller F, Turgeon R. 2003. Symplastic continuity between companion cells and the translocation stream: long-distance transport is controlled by retention and retrieval mechanisms in the phloem. *Plant Physiology* **131,** 1518–1528.

Baker HG, Baker I. 1990. The predictive value of nectar chemistry to the recognition of pollinator types. *Israel Journal of Botany* **39,** 157–166.

Baker HG, Baker I, Hodges SA. 1998. Sugar composition of nectars and fruits consumed by birds and bats in the tropics and subtropics. *Biotropica* **30,** 559–586.

Bradshaw HD, Wilbert SM, Otto KG, Schemske DW. 1995. Genetic mapping of floral traits associated with reproductive isolation in monkeyflowers (*Mimulus*). *Nature* **376,** 762–765.

Chalcoff VR, Aizen MA, Galetto L. 2006. Nectar concentration and composition of 26 species from the temperate forest of South America. *Annals of Botany* **97,** 413–421.

Cronk Q, Ojeda I. 2008. Bird-pollinated flowers in an evolutionary and molecular context. *Journal of Experimental Botany* **59,** 715–727.

De la Barrera E, Nobel PS. 2004. Nectar: properties, floral aspects, and speculations on origin. *Trends in Plant Science* **9,** 65–69.

Eisenreich W, Ettenhuber C, Laupitz R, Theus C, Bacher A. 2004. Isotopolog perturbation techniques for metabolic networks: metabolic recycling of nutritional glucose in *Drosophila melanogaster*. *Proceedings of the National Academy of Sciences, USA* **101,** 6764–6769.

Elias TS, Rozich WR, Newcombe L. 1975. The foliar and floral nectaries of *Turneara ulmifolia* L. *American Journal of Botany* **62,** 570–576.

Elisens WJ, Freeman CE. 1988. Floral nectar sugar composition and pollinator type among new world genera in tribe Antirrhineae (Scrophulariaceae). *American Journal of Botany* **75,** 971–978.

Fahn A. 1979. Ultrastructure of nectaries in relation to nectar secretion. *American Journal of Botany* **66,** 977–985.

Fahn A. 2000. Structure and function of secretory cells. In: Hallahan DL, Gray JC, eds. *Advances in botanical research*, Vol. 31. *Plant trichomes*. Academic Press, 37–75.

Figier J. 1968. Electron microscopic localization of acid phosphatase in extrafloral nectary of *Vicia faba* L. *Planta* **83,** 60–79.

Frey-Wyssling A. 1955. The phloem supply to the nectaries. *Acta Botanica Neerlandica* **4,** 358–369.

Ge YX, Angenent GC, Wittich PE, *et al.* 2000. *NEC1*, a novel gene, highly expressed in nectary tissue of *Petunia hybrida*. *The Plant Journal* **24,** 725–734.

Geigenberger P, Langenberger S, Wilke I, Heineke D, Heldt HW, Stitt M. 1993. Sucrose is metabolized by sucrose synthase and glycolysis within the phloem complex of *Ricinus communis* L. seedlings. *Planta* **190,** 446–453.

Grassmann P. 1884. Die Septaldrüsen: Ihre Verbreitung, Entstehung und Verrichtung. *Flora* **67,** 113–136.

Heidenreich M, Köckenberger W, Kimmich R, Chandrakumar N, Bowtell R. 1998. Investigation of carbohydrate metabolism and transport in castor bean seedlings by cyclic *J*-cross-polarization imaging and spectroscopy. *Journal of Magnetic Resonance* **132,** 109–124.

Hölscher D, Brand S, Wenzler M, Schneider B. 2008. NMR-based metabolic profiling of *Anigozanthos* floral nectar. *Journal of Natural Products* **71,** 251–257.

Kalinowski HO, Berger S, Braun S. 1984. *^{13}C NMR Spektroskopie*. Stuttgart: Thieme.

Kallarackal J, Komor E. 1989. Transport of hexoses by the phloem of *Ricinus communis* L. seedlings. *Planta* **177,** 336–341.

Kleijn RJ, Geertman JMA, Nfor BK, Ras C, Schipper D, Pronk JT, Heijnen JJ, van Maris AJA, van Winden WA. 2007. Metabolic flux analysis of a glycerol-overproducing *Saccharomyces cerevisiae* strain based on GC-MS, LC-MS and NMR-derived ^{13}C-labelling data. *FEMS Yeast Research* **7,** 216–231.

Lüttge U. 1961. Über die Zusammensetzung des Nektars und den Mechanismus seiner Sekretion. 1. *Planta* **56,** 189–212.

Lüttge U. 1962. Über die Zusammensetzung des Nektars und den Mechanismus seiner Sekretion. 3. Die Rolle der Rückresorption und der spezifischen Zuckersekretion. *Planta* **59,** 175–194.

Nicolson SW, Fleming PA. 2003. Nectar as food for birds: the physiological consequences of drinking dilute sugar solutions. *Plant Systematics and Evolution* **238,** 139–153.

Öpik H, Rolfe S. 2005. *The physiology of flowering plants*. Cambridge: Cambridge University Press.

Pacini E, Nepi M, Vesprini JL. 2003. Nectar biodiversity: a short review. *Plant Systematics and Evolution* **238,** 7–21.

Ratcliffe RG, Shachar-Hill Y. 2006. Measuring multiple fluxes through plant metabolic networks. *The Plant Journal* **45,** 490–511.

Razem FA, Davis AR. 1999. Anatomical and ultrastructural changes of the floral nectary of *Pisum sativum* L. during flower development. *Protoplasma* **206,** 57–72.

Simpson MG. 1993. Septal nectary anatomy and phylogeny of the Haemodoraceae. *Systematic Botany* **18,** 593–613.

Stuurman J, Hoballah ME, Broger L, Moore J, Basten C, Kuhlemeier C. 2004. Dissection of floral pollination syndromes in *Petunia*. *Genetics* **168,** 1585–1599.

Viola R, Davies HV, Chudeck AR. 1991. Pathways of starch and sucrose biosynthesis in developing tubers of potato (*Solanum tuberosum* L.) and seeds of faba bean (*Vicia faba* L.). *Planta* **183,** 202–208.

Wolff D. 2006. Nectar sugar composition and volumes of 47 species of Gentianales from a southern Ecuadorian montane forest. *Annals of Botany* **97,** 767–777.

Ziegler H. 1956. Untersuchungen über die Leitung und Sekretion der Assimilate. *Planta* **47,** 447–500.

Zimmermann M. 1953. Papierchromatographische Untersuchungen über die pflanzliche Zuckersekretion. *Bericht der Schweizerischen Botanischen Gesellschaft* **63,** 402–429.